

# Black Hole Discharge: very-high-energy gamma rays from black hole-neutron star mergers

Zhen Pan<sup>1,\*</sup> and Huan Yang<sup>1,2,†</sup>

<sup>1</sup>*Perimeter Institute for Theoretical Physics, ON, N2L2Y5, Canada*

<sup>2</sup>*University of Guelph, Guelph, Ontario N2L 3G1, Canada*

(Dated: May 14, 2019)

With mass ratio larger than  $\sim 5$ , star disruption is not expected for a black hole merging with a neutron star during the final plunge phase. In the late inspiral stage, the black hole is likely charged as it cuts through the magnetic field carried by the neutron star, leaving a temporarily charged black hole after merger. The unstable charged state of the remnant black hole rapidly neutralizes by interacting with the surrounding plasma and photons, which we investigate in first principle by numerically solving a coupled set of Boltzmann equations. The resulting basic picture is as follows. Electrons and positrons are accelerated in the BH electric field, which then lose energy to surrounding soft photons via Compton scattering; more electrons and positrons will be created from pair production as the hard photons colliding with soft photons, or through the Schwinger process in strong electromagnetic fields. The cascade stops when the charged black hole accretes enough opposite charges and becomes neutralized. We find that  $\sim 10\%$  (which depends on the soft photon energy and number density) of the total electric energy is carried away to infinity in a time interval  $\sim 1$  ms by very-high-energy ( $> 50$  GeV, the low energy detection threshold of the MAGIC telescope) gamma rays whose spectrum is approximately a power law with spectral index  $\sim -2.3$ .

**Introduction.** Short gamma-ray burst (sGRB) has long been suggested to be associated with double neutron star (NS) mergers - a conjecture lately supported by the multi-messenger detection of gravitational waves (GWs) and various electromagnetic (EM) counterparts in GW170817 [1, 2]. Another possible origin of sGRBs is merging black hole (BH) and NS binary. If the BH disrupts the NS during the late inspiral phase, the remnant matter may form a temporary accretion disk around the final BH and power an energetic jet along with gamma ray emission [3]. This scenario may be tested with imminent detection of BH/NS merger events in the O3 run of LIGO/Virgo collaboration, together with EM observations. Future third-generation GW detectors may be able to probe the NS disruption [4, 5] and help distinguish possible low-mass BH/NS binaries from binary NSs [6].

On the other hand, if the BH/NS binary mass ratio is beyond certain threshold  $\sim 5$  ([7], dubbed as type III merger therein and hereafter), no star disruption is expected. The BH basically swallows the NS, and the post-merger waveform is dominated by BH ringdowns [8]. The associated electromagnetic emission during the merger mainly originates from the surrounding plasma within the system, which has a much smaller energy reservoir than a typical sGRB. A few mechanisms that might lighten up these systems have been proposed, e.g., DC circuit [9, 10], BH pulsar [11] and BH electric generator [12]. Previous discussions focused on estimating the energy budget rather than description about the plasma dynamics and emission properties, so that the spectroscopic prediction of EM counterparts has not been made.

In this *Letter*, we report a first-principle study of EM signals from the aftermath of type III BH/NS mergers. Considering a typical NS mass  $\sim 1.4M_{\odot}$ , the correspond-

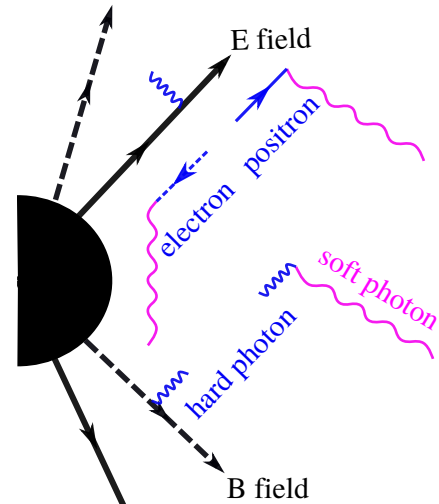


FIG. 1. A cartoon picture summarizing major reactions in our model: electrons and positrons are accelerated in opposite directions by the electric field; soft photons gain energy via IC scatterings with electrons and positrons;  $e^{\pm}$  pairs are created as hard photons colliding with background soft photons, or through Schwinger process in electromagnetic fields. Vacuum polarization in charged BHs was originally considered in [13].

ing BH mass threshold is already near the lower end of the observed BH mass in X-ray binaries [14–17]. To simplify the set-up, we neglect the BH spin and assume the final BH to be Schwarzschild. The amount of electric charge carried by the BH can be roughly estimated as

(also see [11])  $Q \approx EM^2 \approx B_{\text{NS}} r_{\text{NS}}^2$ , where  $M$  is BH mass and  $E \sim (v_{\text{rel}}/c)B_{\text{NS}} \approx B_{\text{NS}}$  is the magnitude of the induced electric field. To get an intuition about the BH charge  $Q$ , we define a dimensionless quantity

$$\Gamma_Q \equiv \frac{Qe}{Mm_e}, \quad (1)$$

which is the ratio of electric force and gravitational force on an electron outside the charge BH. For  $M = 10M_\odot$ ,  $B_{\text{NS}} = 10^{12}$  G and  $r_{\text{NS}} = 10$  km, we have  $\Gamma_{Q,12} \approx 4 \times 10^{14}$  and total electric energy  $Q_{,12}^2/4M \approx 10^{42}$  ergs, where the lower index  $_{12}$  is the power index of  $B_{\text{NS}}$  [G]. Electrons and positrons are accelerated in the BH electric field, which consequently produce hard photons via inverse Compton (IC) scattering with surrounding soft photons. More electrons and positrons will be generated as a result of pair production of the hard photons interacting with soft photons and electromagnetic fields (see Fig. 1). The above cascade stops only when the charged BH neutralizes by accreting enough opposite charges. As we will show later  $\sim 10\%$  of the total energy is carries away by  $\sim 10^{41}$  gamma-ray photons with energy  $> 50$  GeV, which is the low-energy detection threshold of the MAGIC telescope [18].

We use geometric units  $G = c = 1$  and the Schwarzschild metric is written as

$$ds^2 = -\alpha^2 dt^2 + \alpha^{-2} dr^2 + r^2 d\Omega^2, \quad (2)$$

where  $\alpha := \sqrt{1 - 2M/r}$  and we assume  $M = 10M_\odot$  in this paper. Tortoise coordinate  $r_* \equiv r + 2M \ln | \frac{r}{2M} - 1 |$  is used in our numerical simulations.

**Governing Equations.** The single particle distribution function  $f(t, r, p)$  in phase space is defined by counting the particle number  $dN$  within the volume  $(r, r+dr)$  and  $(p, p+dp)$ :  $dN = f(t, r, p) 4\pi \alpha^{-2} dr dp = f(t, r, p) 4\pi dr_* dp$ , where  $p$  is the contravariant component of momentum in the  $r$  direction  $p \equiv p^r = \sqrt{(p_t)^2 - \alpha^2 m^2}$ , with  $-p_t$  being the particle energy measured by observers at infinity and  $m$  being the particle mass. Boltzmann equation in the covariant form is written as [e.g., 19]

$$p^\mu \frac{\partial f}{\partial x^\mu} + p^i \frac{\partial f}{\partial p^i} + e F^{\mu\nu} p_\nu \frac{\partial f}{\partial p^\mu} = C[f], \quad (3)$$

where  $F^{\mu\nu}$  is the Maxwell tensor;  $\mu, \nu$  are spacetime indices and  $i$  is a spatial index. For the system of spherical symmetry we are considering, the Boltzmann equations for distribution functions of electrons  $f_+(t, r, p_+)$ , positrons  $f_-(t, r, p_-)$  and hard photons  $f_\gamma(t, r, p_\gamma)$  are written as

$$\begin{aligned} \partial_t f_+(p_+) + v(p_+) \partial_{r_*} f_+(p_+) + a_+ \partial_p f_+(p_+) &= C_+, \\ \partial_t f_-(p_-) + v(p_-) \partial_{r_*} f_-(p_-) + a_- \partial_p f_-(p_-) &= C_-, \\ \partial_t f_\gamma(p_\gamma) + v(p_\gamma) \partial_{r_*} f_\gamma(p_\gamma) &= C_\gamma, \end{aligned} \quad (4)$$

where  $v(p) = p/(-p_t)$ ;  $a_\pm = \pm \alpha^2 N_Q e^2 / r^2 m_e$  are the acceleration of positrons and electrons in the electric field,

with  $N_Q(r)e$  being the total charge enclosed by radius  $r$ . The collision terms  $C_{\pm, \gamma}$  are contributed by IC scatterings and pair productions (see Fig. 1),

$$\begin{aligned} C_+ &= -\mathcal{R}_{\text{IC}}(p_+) f_+(p_+) + \mathcal{R}_{\text{IC}}(p_+^{\text{old}}) f_+(p_+^{\text{old}}) \frac{dp_+^{\text{old}}}{dp_+} \\ &\quad + \mathcal{R}_{\text{pair}}(p_\gamma^{\text{old}}) f_\gamma(p_\gamma^{\text{old}}) \frac{dp_\gamma^{\text{old}}}{dp_+}, \end{aligned} \quad (5a)$$

$$\begin{aligned} C_- &= -\mathcal{R}_{\text{IC}}(p_-) f_-(p_-) + \mathcal{R}_{\text{IC}}(p_-^{\text{old}}) f_-(p_-^{\text{old}}) \frac{dp_-^{\text{old}}}{dp_-} \\ &\quad + \mathcal{R}_{\text{pair}}(p_\gamma^{\text{old}}) f_\gamma(p_\gamma^{\text{old}}) \frac{dp_\gamma^{\text{old}}}{dp_-}, \end{aligned} \quad (5b)$$

$$\begin{aligned} C_\gamma &= -\mathcal{R}_{\text{pair}}(p_\gamma) f_\gamma(p_\gamma) + \mathcal{R}_{\text{IC}}(p_+^{\text{old}}) f_+(p_+^{\text{old}}) \frac{dp_+^{\text{old}}}{dp_\gamma} \\ &\quad + \mathcal{R}_{\text{IC}}(p_-^{\text{old}}) f_-(p_-^{\text{old}}) \frac{dp_-^{\text{old}}}{dp_\gamma}, \end{aligned} \quad (5c)$$

where  $\mathcal{R}_{\text{IC}}$  is the Compton scattering rate of a lepton in the soft photon background, and  $\mathcal{R}_{\text{pair}}$  is the total pair production rate of a hard photon colliding with soft photons and through Schwinger process in strong electromagnetic fields ( $\gamma^{\text{hard}} + \gamma^{\text{soft}}/E/B \rightarrow e^+ + e^-$ ), i.e.,  $\mathcal{R}_{\text{pair}} = \mathcal{R}_{\gamma\gamma} + \mathcal{R}_{\gamma E} + \mathcal{R}_{\gamma B}$ . On the right hand side of Eq. (5a),  $p_+^{\text{old}}$  is the momentum of positrons that slow down to  $p_+$  after one IC scattering;  $p_\gamma^{\text{old}}$  is the momentum of hard photons that annihilate into an  $e^\pm$  pairs with momentum  $p_+$ . In Eqs. (5b,5c),  $p_{\pm, \gamma}^{\text{old}}$  are defined in a similar way.

To close the Boltzmann equations (4), we need the sourced Maxwell's equations

$$\partial_t N_Q = -4\pi \int_{-\infty}^{\infty} v(p) [f_+(p) - f_-(p)] dp, \quad (6a)$$

$$\partial_{r_*} N_Q = 4\pi \int_{-\infty}^{\infty} [f_+(p) - f_-(p)] dp. \quad (6b)$$

**Initial conditions.** The initial distribution functions  $f_{\pm, \gamma}(r, p)$ , electric charge  $Q$  carried by the BH (or equivalently the dimensionless quantity  $\Gamma_Q$ ) and all the reaction coefficients:  $\mathcal{R}_{\text{IC}}, \mathcal{R}_{\gamma\gamma}, \mathcal{R}_{\gamma E}, \mathcal{R}_{\gamma B}$  are specified as follows. For a given  $\Gamma_Q$ , we set  $f_+|_{t=0} = f_\gamma|_{t=0} = 0$  and

$$f_-|_{t=0} dp = \frac{n(r)}{\sqrt{2\pi}\sigma_p} \exp\left(-\frac{(p/\Gamma_Q m_e)^2}{2\sigma_p^2}\right) d\left(\frac{p}{\Gamma_Q m_e}\right),$$

with  $\sigma_p = 0.1$  and  $n(r)/r^2 = c_n / (\exp((r_* - 6M)/2M) + 1)$ , where  $c_n$  is some normalization constant ensuring electric neutrality at infinity. As we will show later, the discharge process and final products mainly depend on the initial amount of total electric energy, while the initial distribution function  $f_-$  does not affect the evolution much as long as the initial kinetic energy of electrons is a minor component.

Motivated by the dipole geometry, we assume an initial magnetic field

$$B(r)|_{t=0} = B_{\text{NS}}(r_{\text{NS}}/r)^3 \quad (\text{for } r > r_c = 6M). \quad (7)$$

The soft photon energy and number density are estimated assuming they mainly come from cyclotron radiation by the non-relativistic leptons (with Goldreich-Julian density [20]) in the magnetic field, i.e.,

$$E_\gamma^{\text{soft}} = \hbar\omega_B = \hbar \frac{eB}{m_e}, \quad (8)$$

$$n_\gamma^{\text{soft}}(r) \approx \int_{r_c}^{\infty} n_{\text{GJ}}(r') f_{\text{cyc}}(r') \frac{r'^2}{|\vec{r}' - \vec{r}|^2} dr',$$

where  $n_{\text{GJ}} = 0.07(B/\text{G}) \text{ cm}^{-3}$  is the Goldreich-Julian number density (for a NS magnetosphere with rotation period of 1 sec),  $f_{\text{cyc}} \approx \frac{2}{3} \frac{e^2}{\hbar c} \omega_B$  is the number of soft photons emitted per unit time from a non-relativistic lepton moving in the magnetic field. As a result, we can parameterize the rate of a lepton scattered off soft photons as

$$\mathcal{R}_{\text{IC}} = n_\gamma^{\text{soft}} \sigma_{\text{T}} = (10N_\gamma^{\text{soft}}) \times \alpha^2 r_c^5 / (r_c^5 + r^5) M^{-1}, \quad (9)$$

where  $\sigma_{\text{T}}$  is the Thomson cross section.  $N_\gamma^{\text{soft}}$  is a free parameter of  $O(1)$  and the factor  $\alpha^2$  is included to mimic the lower photon number density in the vicinity of the BH due to BH capturing. The energy of soft photons varies from maximum value  $\sim 10$  eV to zero depending on the magnitude of underlying magnetic field. For our purpose here, only the soft photons at the high-energy end affect both emission and absorption of hard photons. Therefore, we assume all soft photons are of the same energy  $E_\gamma^{\text{soft}} \in [1, 10]$  eV.

For the soft photon background above, the coefficient  $\mathcal{R}_{\gamma\gamma}$  is written as  $\mathcal{R}_{\gamma\gamma} = \xi_{\gamma\gamma}(p, E_\gamma^{\text{soft}})(\sigma_{\gamma\gamma}/\sigma_{\text{T}})\mathcal{R}_{\text{IC}}$ , where  $\sigma_{\gamma\gamma} \approx 0.35\sigma_{\text{T}}$  is the cross section of pair creation  $\gamma + \gamma \rightarrow e^+ + e^-$  [21] and factor  $\xi_{\gamma\gamma}$  takes account of the energy threshold below which this process is prohibited. The pair creation coefficients  $\mathcal{R}_{\gamma E}$  and  $\mathcal{R}_{\gamma B}$  are known as [e.g., 22]

$$\mathcal{R}_{\gamma X} = \frac{0.23}{a_0} X' \exp\left(-\frac{4}{3xX'}\right), \quad (10)$$

where  $X = \{E, B\}$ ,  $a_0$  is the Bohr radius,  $x = p_\gamma/2m_e$ ,  $X' = X/X_{\text{cr}}$  and  $X_{\text{cr}} \equiv m^2 c^3/\hbar e = 4.4 \times 10^{13}$  G. In our model, we obtain electric field  $E(t, r)$  self consistently and assume the outgoing magnetic field  $B(t, r)$  expands in the light speed. For convenience, we define  $\mathcal{R}_{\gamma 12} = \{\mathcal{R}_{\gamma E}|_{E=(N_Q e/r^2)(\Gamma_Q, 12/\Gamma_Q)}, \mathcal{R}_{\gamma B}|_{B_{\text{NS}}=10^{12}\text{G}}\}$  and similarly for any other  $\mathcal{R}_{\gamma\#}$ .

**BH discharge and very-high-energy gamma rays.** We choose a fiducial model with  $\Gamma_Q = 3 \times 10^8$ ,  $E_\gamma^{\text{soft}} = 10$  eV,  $N_\gamma^{\text{soft}} = 1$ ,  $\{\mathcal{R}_{\gamma E}, \mathcal{R}_{\gamma B}\} = \mathcal{R}_{\gamma 12}$ , and show the detailed discharge process in Fig. 2. In the region where electric field is not screened, electrons and positrons are accelerated and then scattered by soft photons in a distance  $1/\mathcal{R}_{\text{IC}} \sim 0.1M$ . Hard photons produced by IC scatterings are depleted by the electromagnetic fields immediately via Schwinger process  $\gamma + E/B \rightarrow e^+ + e^-$ .

As a result, number of  $e^\pm$  pairs increases exponentially while number of hard photons stays at a relatively low level due to  $\mathcal{R}_{\text{pair}} \gg \mathcal{R}_{\text{IC}}$  (see 1st row of Fig. 2). After a few folds of exponential growth, local number density of pairs exceeds the initial charge density, i.e.,  $n_+ \approx n_- \gg |n_+ - n_-|$ , and electric field is screened by electrons and positrons accelerated in opposite directions (see 2nd row of Fig. 2). As the exponential growth continues, electric field is screened over larger and larger area, leaving a window where EM fields vanish and hard photons survive the Schwinger process. In the EM-free window, leptons and hard photons are driven towards lower energy by colliding with soft photons (see 3rd row of Fig. 2).

We measure number of very-high-energy (VHE) gamma rays escaping to infinity

$$N_\gamma^{\text{VHE}} = 4\pi \int_{p>50\text{GeV}} f_\gamma(t, r, p)|_{r \rightarrow \infty} dt dp, \quad (11)$$

and the energy spectrum  $dN_\gamma^{\text{VHE}}/dp$ . We find the energy spectrum is roughly a power law  $dN_\gamma^{\text{VHE}}/dp \propto p^{-2.3}$  plus a bump at  $p \approx m_e^2/E_\gamma^{\text{soft}}$ , which is the energy threshold of hard photons colliding with soft photons and producing  $e^\pm$  pairs. In Fig. 3, we detail the dependence of  $N_\gamma^{\text{VHE}}$  on the four model parameters, which is approximately described by  $N_\gamma^{\text{VHE}} = N_0(E_\gamma^{\text{soft}}, N_\gamma^{\text{soft}}, B_{\text{NS}}) \times (\Gamma_Q)^2$ , where  $N_0|_{p>50\text{GeV}} \approx 10^{12}$  (and  $N_0|_{p>20\text{GeV}} \approx 3 \times 10^{12}$ ). The initial BH charge sets the total energy budget ( $\propto \Gamma_Q^2$ ) for particle creation, which explains the dependence of  $N_\gamma^{\text{VHE}}$  on  $\Gamma_Q$ . The soft photon energy  $E_\gamma^{\text{soft}}$  sets an threshold  $m_e^2/E_\gamma^{\text{soft}}$  below which hard photons freely stream in the soft photon background without pair creation. Therefore the smaller  $E_\gamma^{\text{soft}}$ , the higher threshold and the more hard photons escaping to infinity. The number density of soft photons  $N_\gamma^{\text{soft}}$  determines the mean free path of leptons ( $1/\mathcal{R}_{\text{IC}}$ ) and that of hard photons ( $1/\mathcal{R}_{\gamma\gamma}$ ), where the former determines the amount of energy a lepton can gain from the electric field and the latter determines the annihilation possibility of a hard photon. Therefore the larger  $N_\gamma^{\text{soft}}$ , the less energy carried away to infinity by VHE photons. The magnetic field strength  $B_{\text{NS}}$  (or equivalently the coefficient  $\mathcal{R}_{\gamma\#}$ ) mainly affects the width of window in which EM fields vanish and hard photons survive the Schwinger process. We expect this to be a marginal effect which is confirmed by our simulations.

**Detection prospect.** For very short observation time, the sensitivity of a Cherenkov telescope is limited by number  $N_{\text{obs}}$  of high-energy particles arriving at the telescope. Using the commonly used detection criteria  $N_{\text{obs}} > 10$  [18], we obtain the horizon distance

$$d = \left(\frac{N_\gamma^{\text{VHE}}}{1.2 \times 10^{41}}\right)^{1/2} \left(\frac{S}{1 \text{ km}^2}\right)^{1/2} \text{ Mpc}, \quad (12)$$

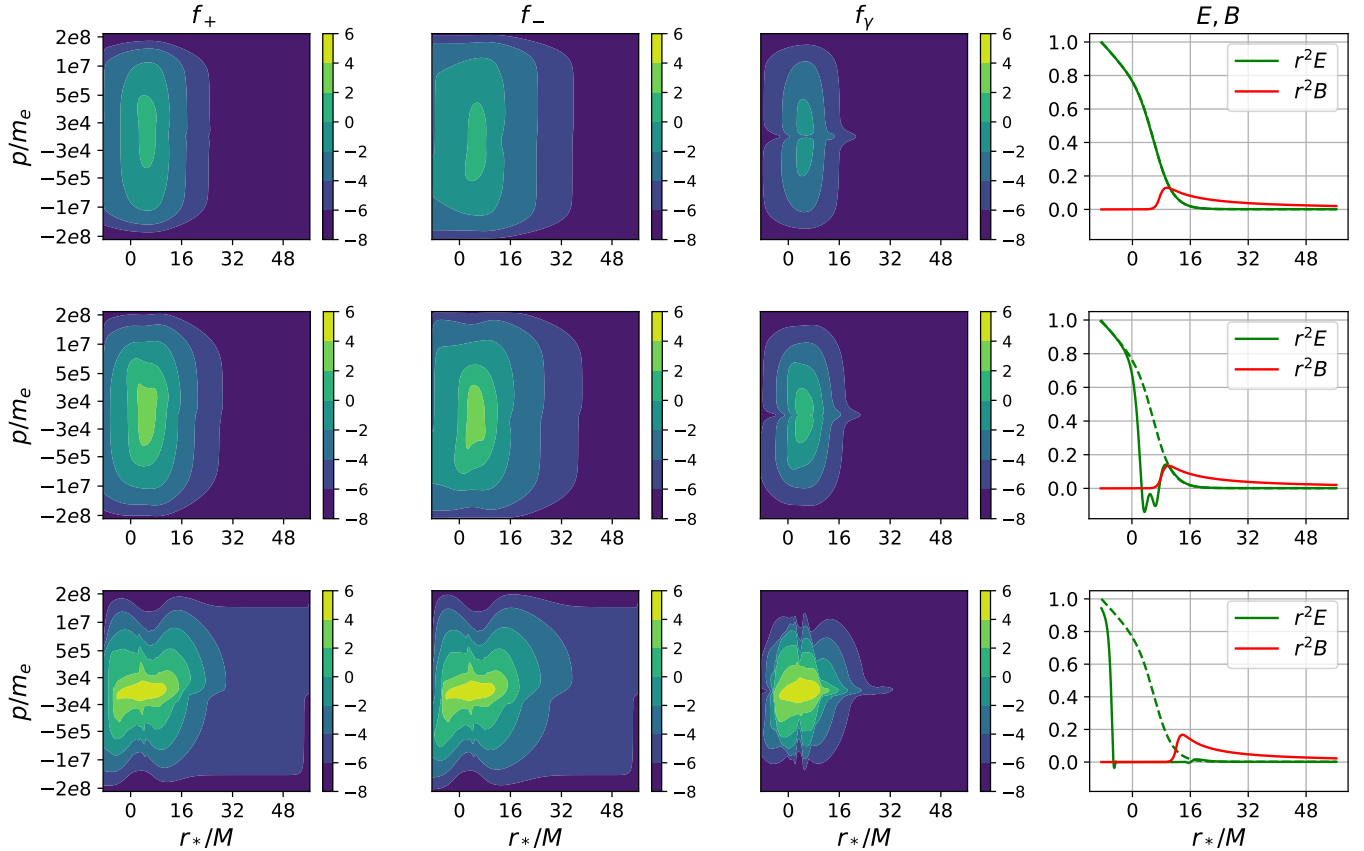


FIG. 2. BH discharge process of a fiducial model with parameters  $\Gamma_Q = 3 \times 10^8$ ,  $E_\gamma^{\text{soft}} = 10$  eV,  $N_\gamma^{\text{soft}} = 1$  and  $\{\mathcal{R}_{\gamma E}, \mathcal{R}_{\gamma B}\} = \mathcal{R}_{\gamma 12}$ . Top/Middle/Bottom rows are snapshots at  $t = 0.2M/0.6M/3.7M$ , respectively. Left three columns are the distribution functions  $f_{\pm, \gamma}$  (more accurately  $\log_{10}[f_{\pm, \gamma} \cdot (M\Gamma_Q m_e)]$ ). Right three panels are EM fields  $r^2E$  and  $r^2B$  in unit of  $M^2 \times 10^{12}G$ , where the dashed lines are the initial value of  $r^2E$ .

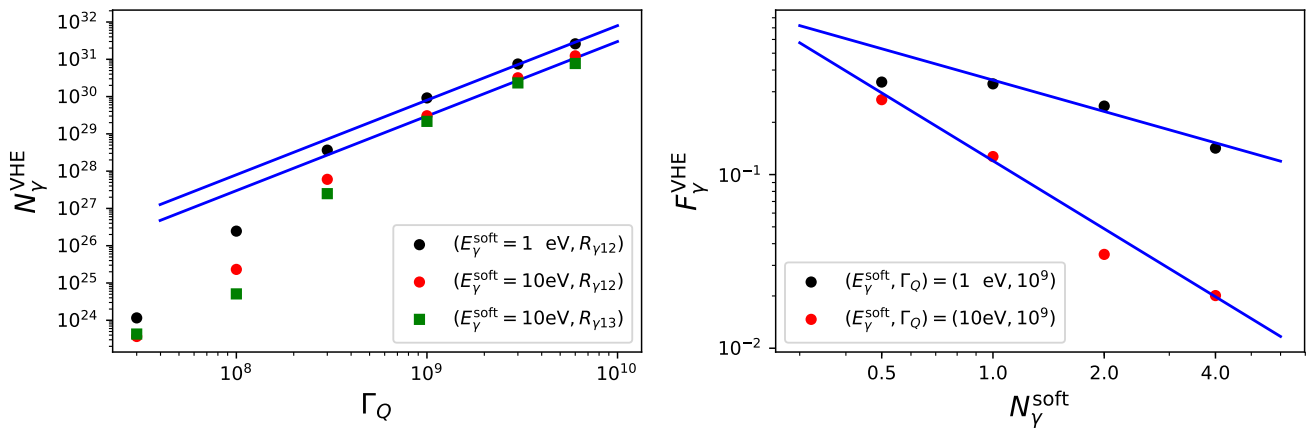


FIG. 3. Dependence of VHE photon number  $N_\gamma^{\text{VHE}}$  on various model parameters, which take fiducial values if not explicitly specified. In the left panel, we show the relation of  $N_\gamma^{\text{VHE}}$  with initial BH charge  $\Gamma_Q$ , which is fitted by  $N_\gamma^{\text{VHE}} = N_0 \times (\Gamma_Q)^2$ , with  $N_0 \approx 10^{12}$ . In the right panel, we show dependence of  $F_\gamma^{\text{VHE}}$  (fraction of initial electric energy carried away to infinity by VHE photons) on soft photon number density  $N_\gamma^{\text{soft}}$ , which is roughly  $F_\gamma^{\text{VHE}} \propto (N_\gamma^{\text{soft}})^{-\xi}$ , with power index  $\xi$  being  $O(1)$ .

within which BH discharge events are visible to the Cherenkov telescope, where the effective area  $S \sim 5\text{km}^2$  for the telescope proposed in [23].

Our simulation is unable to trace the lowest energy photons due to limited resolution. Assuming hard photons of energy 100 MeV carry away total energy  $5 \times 10^{41}$  ergs, the horizon distance for Fermi LAT [24] (with effective area  $\sim 0.35\text{m}^2$  at this energy) is about 0.1 Mpc.

**Summary and discussion.** In this *Letter*, we perform a first-principle study of EM counterparts of type III BH/NS mergers, where the BH is large enough to swallow the NS as a whole without star disruption. In the late inspiral stage, the BH is charged as moving in the NS magnetosphere. The remnant BH neutralizes rapidly via a discharge process, through which the electric energy is converted into the kinetic energy of  $e^+/e^-$  pairs and hard photons. For a typical BH/NS merger with  $M = 10M_\odot$ ,  $B_{\text{NS}} = 10^{12}\text{G}$  and  $r_{\text{NS}} = 10\text{km}$ , we find that  $\sim 10\%$  of the total electric energy is carried away to infinity in a time interval  $\sim 1\text{ms}$  by VHE gamma rays, whose spectrum is approximately a power law  $dN_\gamma^{\text{VHE}}/dp \propto p^{-2.3}$  plus a bump at  $p \approx m_e^2/E_\gamma^{\text{soft}}$ .

We may similarly estimate the EM signal from a BH/magnetar merger. For a magnetar with magnetic field  $10^{15}\text{G}$  [25, 26], the final BH would be charged to  $10^3 Q_{.12}$  with electric energy  $\sim 10^{48}$  ergs. Soft photon energy ( $\hbar\omega_B$ ) would be  $10^3$  larger, and typical hard photon energy  $m_e^2/E_\gamma^{\text{soft}} \sim 25\text{MeV}$ . Therefore we expect a dim sGRB after a BH/magnetar merger which is visible to Fermi LAT within  $\sim 100\text{Mpc}$ . The discharging process discussed here also sheds light on the EM signature of charged BH mergers [27, 28] and/or charged BHs formed through gravitational collapse of magnetized NSs [29].

Throughout this work, we have assumed spherical symmetry for the system of charged BH and surrounding particles, and have solved the Boltzmann equations of  $1+1$  form. To understand the details of 3D discharge process in BH magnetosphere, it is preferable to apply the particle-in-cell simulations [30–32].

**Acknowledgement.** We thank Junwu Huang and Luis Lehner for very helpful discussions. This research was also supported by the Natural Sciences and Engineering Research Council of Canada and in part by Perimeter Institute for Theoretical Physics. Research at Perimeter Institute is supported by the Government of Canada through the Department of Innovation, Science and Economic Development Canada and by the Province of Ontario through the Ministry of Research, Innovation and Science.

---

\* zpan@perimeterinstitute.ca

† hyang@perimeterinstitute.ca

- [1] LIGO/Virgo Scientific Collaboration, *Phys. Rev. Lett.* **119**, 161101 (2017), arXiv:1710.05832.
- [2] LIGO/Virgo Scientific Collaboration, *Astrophys. J.* **848**, L12 (2017).
- [3] H.-T. Janka, T. Eberl, M. Ruffert, and C. L. Fryer, *Astrophys. J.* **527**, L39 (1999), arXiv:9908290 [astro-ph].
- [4] H. Miao, H. Yang, and D. Martynov, *Phys. Rev.* **D98**, 044044 (2018), arXiv:1712.07345 [gr-qc].
- [5] D. Martynov, H. Miao, H. Yang, F. H. Vivanco, E. Thrane, R. Smith, P. Lasky, W. E. East, R. Adhikari, A. Bauswein, *et al.*, arXiv preprint arXiv:1901.03885 (2019).
- [6] H. Yang, W. E. East, and L. Lehner, *Astrophys. J.* **856**, 110 (2018), [Erratum: *Astrophys. J.* 870, no.2, 139 (2019)], arXiv:1710.05891 [gr-qc].
- [7] M. Shibata, K. Kyutoku, T. Yamamoto, and K. Taniguchi, *Phys. Rev. D* **79**, 044030 (2009).
- [8] Z. Mark, H. Yang, A. Zimmerman, and Y. Chen, *Phys. Rev.* **D91**, 044025 (2015), arXiv:1409.5800 [gr-qc].
- [9] S. T. McWilliams and J. Levin, *Astrophys. J.* **742**, 90 (2011), arXiv:1101.1969.
- [10] D. Lai, *Astrophys. J.* **757**, L3 (2012), arXiv:1206.3723 [astro-ph.HE].
- [11] J. Levin, D. J. D’Orazio, and S. Garcia-Saenz, *Phys. Rev. D* **98**, 123002 (2018), arXiv:1808.07887.
- [12] Z. G. Dai, *Astrophys. J. Lett.* **873**, L13 (2019), arXiv:1902.07939.
- [13] G. W. Gibbons, *Commun. Math. Phys.* **44**, 245 (1975).
- [14] B. Tetarenko, G. Sivakoff, C. Heinke, and J. Gladstone, *The Astrophysical Journal Supplement Series* **222**, 15 (2016).
- [15] J. Strader, L. Chomiuk, T. Maccarone, J. Miller-Jones, and A. Seth, *Nature* **490**, 71 (2012), arXiv:1210.0901 [astro-ph.HE].
- [16] L. Chomiuk, J. Strader, T. J. Maccarone, J. C. Miller-Jones, C. Heinke, E. Noyola, A. C. Seth, and S. Ransom, *The Astrophysical Journal* **777**, 69 (2013).
- [17] J. C. A. Miller-Jones *et al.*, *Mon. Not. Roy. Astron. Soc.* **453**, 3918 (2015), arXiv:1509.02579 [astro-ph.HE].
- [18] J. Aleksic, S. Ansoldi, L. Antonelli, P. Antoranz, A. Babic, *et al.*, *Astroparticle Physics* **72**, 76 (2016).
- [19] A. Mezzacappa and R. A. Matzner, *Astrophys. J.* **343**, 853 (1989).
- [20] P. Goldreich and W. H. Julian, *Astrophys. J.* **157**, 869 (1969).
- [21] R. J. Gould and G. P. Schröder, *Phys. Rev.* **155**, 1404 (1967).
- [22] J. K. Daugherty and A. K. Harding, *Astrophys. J.* **273**, 761 (1983).
- [23] The CTA Consortium, arXiv preprint arXiv:1904.12196 (2019), arXiv:1904.12196 [astro-ph.HE].
- [24] W. B. Atwood, A. A. Abdo, M. Ackermann, W. Althouse, *et al.*, *Astrophys. J.* **697**, 1071 (2009), arXiv:0902.1089 [astro-ph.IM].
- [25] P. M. Woods, V. M. Kaspi, C. Thompson, F. P. Gavriil, H. L. Marshall, D. Chakrabarty, K. Flanagan, J. Heyl, and L. Hernquist, *Astrophys. J.* **605**, 378 (2004), arXiv:astro-ph/0310575 [astro-ph].
- [26] S. Mereghetti, J. Pons, and A. Melatos, *Space Sci. Rev.* **191**, 315 (2015), arXiv:1503.06313 [astro-ph.HE].
- [27] B. Zhang, *The Astrophysical Journal Letters* **827**, L31 (2016).
- [28] T. Liu, G. E. Romero, M.-L. Liu, and A. Li, *The Astrophysical Journal* **826**, 82 (2016).

- [29] A. Nathanail, E. R. Most, and L. Rezzolla, *Mon. Not. Roy. Astron. Soc.* **469**, L31 (2017), arXiv:1703.03223 [astro-ph.HE].
- [30] A. Levinson and B. Cerutti, *Astronomy and Astrophysics* **616**, A184 (2018), arXiv:1803.04427 [astro-ph.HE].
- [31] K. Parfrey, A. Philippov, and B. Cerutti, *Phys. Rev. Lett.* **122**, 035101 (2019), arXiv:1810.03613 [astro-ph.HE].
- [32] A. Y. Chen, Y. Yuan, and H. Yang, *Astrophys. J.* **863**, L31 (2018), arXiv:1805.11039 [astro-ph.HE].